International Journal of Rock Mechanics & Mining Sciences 53 (2012) 18–31

Contents lists available at SciVerse ScienceDirect

International Journal of Rock Mechanics & Mining Sciences

journal homepage: www.elsevier.com/locate/ijrmms

Performance of some distributions to describe rock fragmentation data

José A. Sanchidrián [a,*], Finn Ouchterlony [b], Peter Moser [b], Pablo Segarra [a], Lina M. López [a]

[a] Universidad Politécnica de Madrid—E.T.S.I. Minas, Ríos Rosas 21, 28003 Madrid, Spain
[b] Montanuniversität Leoben, Franz-Josef-Straße 18, A-8700 Leoben, Austria

ARTICLE INFO

Article history:
Received 2 October 2011
Received in revised form
28 March 2012
Accepted 3 April 2012
Available online 21 April 2012

Keywords:
Rock fragmentation
Size distribution
Blasting
Crushing
Curve fitting

ABSTRACT

Ten functions (Weibull, Swebrec, Gilvarry, Grady and Lognormal, and their bi-component versions) are fitted to 448 sets of screened fragment size data from blasted and crushed rock. The ordinary least squares criterion has been used for the fits and two minimization techniques have been tested, in both cases running the problem repeatedly with different initial values of the unknown parameters in order to ensure a global minimum. There is a distinct behavior of errors across the passing range, which has been divided in four zones, coarse ($>80\%$), central (80%–20%), fine (20%–2%) and very fine ($<2\%$). The representation of fragmentation data by some of the distributions can be made with good accuracy in the coarse and central zones, with moderate accuracy in the fine zone and with considerably poor accuracy in the very fine zone. As expected, bi-component distributions generally perform better than the single-components, though there are important differences among them. Extended Swebrec is consistently the best fitting distribution in all zones, with maximum relative errors of less than 25% in the coarse, 15% in the central, and 50% in the fine zones. Bimodal Weibull, bimodal Gilvarry and bimodal Grady's errors are statistically equivalent to extended Swebrec's in the central and fine zones. In the very fine zone, relative errors have a high probability of being in excess of 100%, with maximum expected values being several times that, even for the best fitting functions in this zone. Swebrec is by far the best single component function in all zones, with errors comparable to the best bi-components in the coarse and central.

1. Introduction

The assessment of fragmentation by blasting and by any of the subsequent crushing and grinding stages is important in order to control and optimize the mining operation. Fragmentation characteristics influence the mucking productivity through rock diggability, excavator efficiency, oversize problems and secondary blasting, the crusher throughput and energy consumption, the plant efficiency, yield and recovery, or the price itself of the end product in the case of industrial minerals and aggregates.

Fragment size distributions, or fragmentation distributions, are a statistical representation of the population of fragment, or particle, sizes. Size is, in the context of rock fragmentation, where particles do not have cubical of spherical shape, defined with respect to the smaller square mesh size through which the particle can pass [1,2]. Classical sampling to determine the size distribution would involve measuring the sizes of the particles by any suitable gauge system, build a histogram of sizes and derive a density function of size from the histogram. Of course this is impossible to do with rock fragments' samples, usually involving millions of particles, nor is it the histogram of numbers, or frequencies, of particles of a given size interval that is of interest, but the amount of material in each size interval. In the usual sieving procedure, the mass fraction at each interval of mesh size is obtained, which represents a discrete density function of the amount of mass for each size. The representation of the mass fraction of material with size less than a given mesh is a discrete cumulative distribution. In the case of fragmentation measured from image analysis, it is the particle area, or volume derived from it, that is obtained, and the density or the cumulative functions represent fractions of the total image surface or the estimated volume.

The description of rock fragmentation in the form of a cumulative plot requires a series of pairs of numbers: mesh size and fraction, or percentage, passing. Much can be gained if such data points are substituted by a functional relation, as only a few numbers (the function parameters) are then required to determine any pair of size/fraction passing values. Fragmentation by blasting models [3–11] generally gives predictions for the parameters of a certain size distribution function from which the whole curve (within an acceptable range) can be built. Similarly, the typical output of digital image analysis codes includes, besides a set of size/percentage passing points, the parameters of a distribution function fitting them.

The aim of this work is to assess the ability of ten distribution functions, including some commonly used, to fit experimental

* Corresponding author. Tel.: +34 913367060.
E-mail address: ja.sanchidrian@upm.es (J.A. Sanchidrián).

1365-1609/$ - see front matter © 2012 Elsevier Ltd. All rights reserved.
http://dx.doi.org/10.1016/j.ijrmms.2012.04.001

rock fragmentation data of different origins (blasting, crushing and grinding of different rock and rock-like materials), and features (size and passing ranges, slopes, etc.), in order to determine in what zones of the functions this can be reasonably done, to what extent extrapolation is acceptable, and what errors should be expected. The present work follows on and significantly expands and corrects a preliminary study previously published by the authors [12].

2. Distribution functions for rock fragmentation data

Distributions that describe the sizes of a granular material are typically expressed in the form of cumulative probability, or cumulative distribution functions (CDF), F, giving the probability p that a fragment be smaller than the variable x (i.e. p is the fraction passing a mesh size x):

$$p(x) = F(x,\overline{\pi}) \tag{1}$$

$\overline{\pi}$ being the vector of parameters of the function. The most common distribution function to represent rock fragments from either blasting or mechanical comminution is the Rosin–Rammler, or Weibull [13–15], hereinafter-abbreviated WRR. It is a two-parameter distribution whose cumulative distribution function F_{WRR}, is

$$F_{WRR}(x,x_c,n) = 1-\exp[-(x/x_c)^n] = 1-2^{-(x/x_{50})^n}, \quad 0 \le x \le \infty \tag{2}$$

where x_c is the scale parameter (size at which the fraction passing is $1-1/e$) and n is the shape or uniformity parameter; the second form in Eq. (2) (with base 2) uses the median size x_{50} as scale parameter. The WRR's CDF has an asymptote $F_{WRR}=1$ at large sizes and tends to a power distribution with an exponent n at small sizes:

$$\lim_{x\to 0}\frac{d\ln F_{WRR}}{d\ln x} = n \tag{3}$$

The WRR distribution, originally used by Rosin and Rammler to describe the size distribution of particles generated by crushing, grinding and milling, has also been extensively used to describe rock fragmentation by blasting and is a classical distribution of choice in fragmentation by blasting formulae, that predict the WRR parameters from blast design data [3,4,6,10].

Ouchterlony [16,17] showed that the use of the WRR function has some inadequacies both in the coarse and the fine zones, as (i) there is in practice a maximum fragment size (x_{max}, for which the fraction passing p is 1) whereas the WRR function has an asymptote there, and (ii) the fines tail does not display a linear behavior in a log–log diagram, except possibly in the ultra-fine region. In order to solve this, a three-parameter distribution (the Swebrec function, abbreviated here SWE) was proposed. The Swebrec CDF is

$$F_{SWE}(x,x_{max},x_{50},b) = \frac{1}{1+[\ln(x_{max}/x)/\ln(x_{max}/x_{50})]^b}, \quad 0 < x \le x_{max} \tag{4}$$

where x_{max} is the maximum size (for which $p=F_{SWE}=1$), x_{50} is the median size and b is a shape or undulation parameter. The Swebrec slope tends slowly to zero for small x:

$$\lim_{x\to 0}\frac{d\ln F_{SWE}}{d\ln x} = 0 \tag{5}$$

A third distribution to be assessed is Gilvarry's [18,19], here abbreviated GIL, originally used for describing single fragmentation of brittle bodies and further applied for describing the fragmentation statistics under high-velocity impact [20] and under a variety of other situations, including blasted rock [21]. The Gilvarry is a three-parameter distribution whose CDF is

$$F_{GIL}(x,x_1,x_2,x_3) = 1-\exp\{-[(x/x_1)+(x/x_2)^2+(x/x_3)^3]\}, \quad 0 \le x \le \infty \tag{6}$$

where x_1, x_2, and x_3 are related to the densities of cracks of linear, planar or volume type, respectively. The small-size limit is power-like with unit exponent though in many cases one or more of the x_1, x_2, and x_3 are very large so that, for the practical size range, the log slope at small sizes can be between 1 and 3. At large x it has an $F=1$ asymptote.

Another distribution is Grady's [22,23], abbreviated here GRA, aimed at describing the fragmentation controlled by Griffith cracks always present in solids. The Grady's CDF is a power-exponential expression:

$$F_{GRA}(x,x_g,\alpha) = 1-[1+(x/x_g)^\alpha]\exp[-(x/x_g)^\alpha], \quad 0 \le x \le \infty \tag{7}$$

in which x_g and α are scale and shape parameters, similar to x_c and n of the Weibull. The behavior of the Grady distribution in the extremes is similar to the WRR; for a given shape parameter, it tends to zero for small x twice as fast as the Weibull:

$$\lim_{x\to 0}\frac{d\ln F_{GRA}}{d\ln x} = 2\alpha \tag{8}$$

The lognormal distribution has also been tested:

$$F_{LGN}(x,x_m,s) = \frac{1}{s\sqrt{2\pi}}\int_0^x \frac{1}{t}\exp\left[-(\ln t-x_m)^2/2s^2\right]dt, \quad 0 \le x \le \infty \tag{9}$$

where x_m and s are the location and scale parameters (the mean and the standard deviation of the natural logarithm of x), respectively. Kolmogorov proved that if a particle is broken successively and if each breakage event produces a random number of fragments having random sizes, then, if there is no preferential selection of sizes for breakage, the distribution of particle sizes will tend to the log-normal distribution after many successive fracture events [1]. The lognormal cumulative distribution has an $F=1$ asymptote at large x and the log–log slope increases indefinitely as x goes to zero.

WRR, GIL, GRA and LGN are usually unimodal distributions; SWE may or may not have a mode, depending on the parameters (though it always has a degenerate mode at $x=0$, and has second one at $x=x_{max}$ if $b<1$).

Where the fragment size covers a wide range, data may not be well represented by a single distribution as the above, this being explained in many cases by the different mechanisms of fragments generation: early stage cracking under explosive loading—itself with different modes of fracture at macro and micro scales and in different zones around the borehole [24,25]—and breaking of already formed fragments in collisions with other. It has also been shown that the branching, bifurcation and merging of the cracks lead to a superposition of distributions rather than to a single form [26] and that the granular structure of rock introduces an effective small-size cutoff to any distribution applying to the coarser range [27].

Bimodal distributions can be formed from the unimodal distributions above:

$$F_{Bi}(x,\overline{\pi}_1,\overline{\pi}_2,f) = (1-f)F(x,\overline{\pi}_1)+fF(x,\overline{\pi}_2), \quad 0 \le x \le \infty \tag{10}$$

where F is any of the functions in Eqs. (2), (6), (7) or (9); f is the fraction of the modality with a parameter set, so that $1-f$ is the fraction of the modality. For the Swebrec case, no such bi-component combination has been formed, though a so-called extended version exists that serves a similar purpose:

$$F_{ExSWE}(x,x_{max},x_{50},b,a,c) = \left\{1+a\left[\frac{\ln(x_{max}/x)}{\ln(x_{max}/x_{50})}\right]^b+(1-a)\left[\frac{(x_{max}/x)-1}{(x_{max}/x_{50})-1}\right]^c\right\}^{-1}, \quad 0 < x \le x_{max} \tag{11}$$

whose behavior at large x is that of Eq. (4) and at small x is that of a power distribution with exponent c:

$$\lim_{x\to 0}\frac{d\ln F_{ExSWE}}{d\ln x}=c \tag{12}$$

The extended Swebrec can have one or two modes and also a degenerate one at $x=x_{max}$ if $b<1$. We shall refer generically as single-component to the WRR, SWE, GIL, GRA and LGN, and as bi-component to the bimodal WRR, GIL, GRA and LGN, plus the extended SWE.

The bimodal WRR was used by Djordjevic [8] in his two-component model. The bimodal lognormal has been used with apparently good results to fit rock fragments data by Blair [28]. The lognormal distribution has also been used by Sanchidrián et al. [29] to fit data sets from image analysis.

3. Fragmentation data

The fragment size data used comprises 448 curves, or data sets (Fig. 1), spanning a wide range of sizes and with variable characteristics and origins; they are all obtained by sieving (for the purposes of the present work, data obtained by other methods such as image analysis have not been considered due to its limited reliability in absolute terms but, perhaps, for the coarse sizes). Tables 1a and 1b give a summary of the data used. For each data source, the range of the number of data points of each data set, n_p, the ranges of minimum and maximum sizes, x_{min} and x_{max}, and the ranges of the minimum percentage passing are given, together with the following dimensionless ratios: log size range: $r_x=\log_{10}(x_{max}/x_{max})$; log passing range: $r_p=\log_{10}(p_{max}/p_{max})$ and overall log slope: $s_L=r_p/r_x$. Values given in Table 1 are the extremes of these for each referenced source of data sets.

There is very little rock fragmentation data below 63 μm obtained by dry sieving; lab crushed and milled material [52] goes down to 40 μm; Grimshaw's [36] lab scale blasts were measured down to 2 μm, the fine material by a sedimentation method, but this is exceptional. Sieving in the fine region may contain errors since some material is inevitably lost: in lab blasting this is about 2% according to our experience; in full scale blasting, a lot of the finer material is lost to the atmosphere and deposited away from the sampling area.

Fig. 2 shows the box plots for the entire size and passing data, maximum and minimum of sizes and passings, log ranges in size and passing, and overall log slope of the data sets organized in the six categories of materials in Tables 1a and 1b (1—blasted, mine, through 6—crusher and mill, OCS). The boxes are represented with the common criterion that their upper and lower limits are the 1st and 3rd quartiles and the central (red) line is the median; whiskers outside the box extend a length 1.5 times the inter-quartile range (which corresponds to a 99.3% coverage if the data are normally distributed); values outside are represented as crosses. The notches about the median represent estimates of the confidence intervals of that.

The groups 1 through 6 formed have been tested for similarity in the characteristics shown in Fig. 2 using the Mann-Whitney U test [54], in order to verify how different they are; for all possible pairs of groups, the hypothesis that the distributions of each of their seven variables in Fig. 2 are identical with equal medians is assessed to a 5% significance level. The result is summarized in Table 2, where the parameters shown are the ones for which the comparison test does not reject the hypothesis of equal distributions. No pair of groups has equal distributions for all parameters; the pair of groups with more similarities appear to be 2 (blasted material, lab) and 4 (secondary and tertiary crusher) where the distributions of the whole size and passing values, maximum and minimum sizes and passings, and log passing ranges, cannot be said to be different (while log size ranges and overall log slopes are). Therefore the six groups, fully meaningful as from their origin, have been retained for analysis.

4. Distribution fitting

The five functions in Eqs. (2), (4), (6), (7)and (9), and their bi-component versions, Eqs. (10) and (11), have been fitted to the 448 data sets. Each of these comprises a number of (x_i, p_i) values. Let the distribution functions be written in general form $F_{FUN}(x,\overline{\pi})$, with $\overline{\pi}$ being the vector of parameters (i.e. the unknown variables to be determined in the fitting process), the size of which is n_v ($n_v=2$ for WRR, GRA and LGN, $n_v=3$ for SWE and GIL, $n_v=5$ for

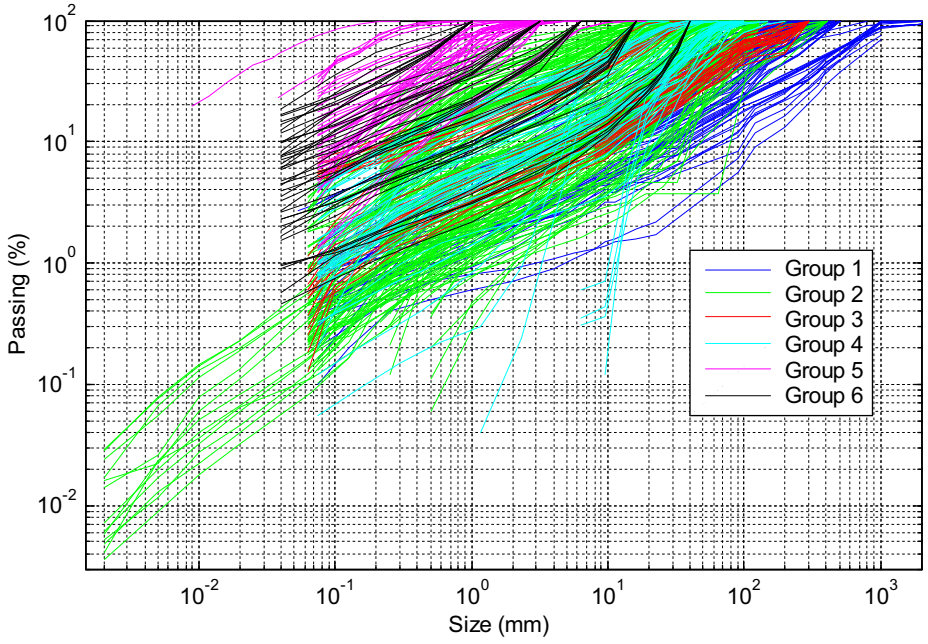

Fig. 1. Fragmentation data. Groups of data 1–6 are defined in Tables 1a and 1b.

Table 1a
Fragmentation data: blasted material.

Mine or quarry site, or rock origin	Rock	No. of sets	Ref.	n_p	x_{min} (mm)	x_{max} (mm)	p_{min} (%)	r_x	r_p	s_L
1 Blasted, mine (78 data sets)										
El Alto, Spain	Limestone	1	[30]	16	0.063	800	0.36	4.1	2.4	0.6
Christmas mine, USA	Copper ore	3	[31]	10	19.05	381	12.1–19.9	1.3	0.7–0.9	0.5–0.7
Mt. Coot-tha, Australia	Hornfel	1	[32]	24	0.355	2000	2.75	3.8	1.6	0.4
Bårarp, Sweden	Granite	7	[33]	19–20	0.075	500–1000	0.1–0.6	3.8–4.1	2.2–2.9	0.5–0.7
Kållered, Sweden	Gneiss	6	[34]	17	0.075	2000	0.34–0.49	4.4	2.3–2.5	0.5–0.6
Billingsryd, Sweden	Dolerite	6	[34]	18	0.074	2000	0.76–1.03	4.4	2.0–2.1	0.4–0.5
South Africa	Gold reef	8	[35]	8–26	0.053–0.075	300–304	0.16–3.1	3.6–3.8	1.5–2.8	0.4–0.8
South Africa	Granite	17	[35]	7	10	500	4.7–12.5	1.7	0.9–1.3	0.5–0.8
Rolla, USA	Dolomite	29	[6]	6–8	9.525	229–457	7.9–20.6	1.4–1.7	0.7–1.1	0.5–0.7
2 *Blasted, specimens (197 data sets)*										
Not reported	Limestone	1	[36]	15	0.002	203	0.0041	5.0	4.4	0.9
Darley Dale, UK	Sandstone	12	[36]	16	0.002	406	0.0035–0.029	5.3	3.5–4.5	0.7–0.8
Imberg, Germany	Sandstone	3	[37]	19–21	0.063	80–125	0.13–0.45	3.1–3.3	2.3–2.8	0.7–0.8
Eibenstein, Austria	Amphibolite	15	[38]	14–20	0.063	25–125	0.14–3.55	2.6–3.3	1.4–2.8	0.5–0.9
Bårarp, Sweden	Granite	7	[33,39]	15–21	0.063	31.5–125	0.21–3.20	2.7–3.3	1.5–2.7	0.6–0.8
El Alto, Spain	Limestone	12	[38]	14–21	0.063	25–125	0.13–4.00	2.6–3.3	1.4–2.9	0.5–0.9
Klinthagen, Sweden	Limestone-stroma[a]	9	[38]	15–20	0.063	31.5–100	0.18–1.86	2.7–3.2	1.7–2.7	0.6–0.9
Klinthagen, Sweden	Limestone-crin[a]	9	[38]	13–21	0.063	20–125	0.16–1.89	2.5–3.3	1.7–2.8	0.6–0.9
Klinthagen, Sweden	Limestone-mass[a]	9	[38]	14–21	0.063	25–125	0.20–2.66	2.6–3.3	1.6–2.7	0.6–0.9
Klinthagen, Sweden	Limestone-frag[a]	10	[38]	13–20	0.063	20–100	0.32–3.41	2.5–3.2	1.5–2.5	0.6–0.8
Norway	Syenite, granite, gabbro, gneiss	21	[40,41]	9–11	0.25–0.50	100–150	0.06–1.85	2.3–2.8	1.7–3.2	0.7–1.3
–	Magnetite concrete	86	[42]	7–13	0.063–0.212	11.3–128	0.26–17.6	1.7–3.3	0.8–2.6	0.4–0.9
–	Cement mortar	3	[43,44]	12	0.075	128	0.10–0.17	3.2	2.8–3.0	0.8–0.9

[a] Limestone qualities in Klinthagen. Stroma: stromatoporoid; crin: crinoidal; mass: massive reef; frag: fragmented.

Table 1b
Fragmentation data: Crushed and milled material.

Mine or quarry site, or rock origin	Rock, equipment	No. of sets	Ref.	n_p	x_{min} (mm)	x_{max} (mm)	p_{min} (%)	r_x	r_p	s_L
3 Primary crusher (42 data sets)										
El Alto, Spain	Limestone, toothed roller crusher	1	[30]	17	0.063	63	1.14	3.0	1.9	0.6
Kållered, Sweden	Gneiss	10	[34]	14	0.074	40	4.9–7.4	2.7	1.1–1.3	0.4–0.5
Tampomas, Indonesia	Andesite, jaw crusher	2	[45]	20–21	0.075	200–300	0.47–1.06	3.4–3.6	2.0–2.3	0.6–0.6
Klinthagen, Sweden	Limestone, toothed roller crusher	28	[46]	9–18	0.063–8	200–300	0.13–18.8	1.4–3.7	0.7–2.9	0.5–0.8
Not reported	Crusher	1	[47]	10–10	1.18	31.5	11.2	1.4	1.0	0.7
4 Secondary and tertiary crusher (50 data sets)										
Norway	Anorthosite, gyratory crusher	4	[41,48]	12	0.075	32	0.60–0.81	2.6	1.6–1.7	0.6
Tampomas, Indonesia	Andesite, gyratory crusher	15	[45]	16–20	0.075	63–200	0.20–1.6	2.9–3.4	1.8–2.7	0.6–0.9
Tampomas, Indonesia	Andesite[a]	31	[45]	8–18	0.075–9.5	28–100	0.04–4.4	1.0–3.1	1.4–3.4	0.5–2.9
5 Mill (43 data sets)										
Tampomas, Indonesia	Andesite, rod mill	9	[45]	9–12	0.075	6.3–19	1.05–6.2	1.9–2.4	1.2–2.0	0.6–0.8
Not reported	AG mill	1	[47]	12	0.038	1.4	23.3	1.6	0.6	0.4
Not reported	Hydrocyclone overflow	1	[47]	12	0.009	0.3	19.5	1.5	0.7	0.5
McCoy mine, USA	Limestone, single particle roll mill	16	[49–51]	12	0.074	3.36	4.1–12.7	1.7	0.9–1.4	0.5–0.8
McCoy mine, USA	Limestone, ball mill	16	[49,50]	11–12	0.074	2.38–3.36	8.3–34.6	1.5–1.7	0.5–1.1	0.3–0.7
6 Crusher and mill (OCS[b]) (38 data sets)										
Eibenstein, Austria	Amphibolite	13	[52]	5–13	0.04	1–40	0.57–18.6	1.4–3.0	0.7–2.2	0.5–0.8
El Alto, Spain	Limestone	5	[52]	5–13	0.04	1–40	0.46–11.7	1.4–3.0	0.9–2.3	0.7–0.8
Klinthagen, Sweden	Limestone-stroma[c]	5	[52]	5–13	0.04	1–40	0.98–14.0	1.4–3.0	0.9–2.0	0.6–0.7
Klinthagen, Sweden	Limestone-crin[c]	5	[52]	5–13	0.04	1–40	0.91–16.9	1.4–3.0	0.8–2.0	0.5–0.7
Klinthagen, Sweden	Limestone-mass[c]	5	[52]	5–13	0.04	1–40	0.94–14.6	1.4–3.0	0.8–2.0	0.6–0.7
Klinthagen, Sweden	Limestone-frag[c]	5	[52]	5–13	0.04	1–40	2.0–16.2	1.4–3.0	0.8–1.7	0.5–0.6

[a] Different materials sampled in the crushing plant have been included in this group: gyratory crusher product mixed with cone crusher recycled product, impact crusher feed (cone product partially sieved off) and product, and product partially sieved off (feed to a rod mill).
[b] Steiner's [53] "optimized comminution sequences", consisting of several stages of crushing and milling with a small scale reduction plus classification and feedback.
[c] Limestone qualities in Klinthagen. Stroma: stromatoporoid; crin: crinoidal; mass: massive reef; frag: fragmented.

BiWRR, ExSWE, BiGRA and BiLGN, and $n_v=7$ for BiGIL); the passing values p_i calculated at a given size x_i from one of the distributions are $p_i^*=F_{FUN}(x_i,\overline{\pi})$.

An ordinary least squares scheme has been used to calculate the vector of parameters; $\overline{\pi}$ is the solution of:

$$\min S(\overline{\pi}) = \min \sum_{i=1}^{n_p} [p_i^*(x_i,\overline{\pi}) - p_i]^2 \quad (13)$$

where n_p is the number of points of a data set. Where there is a wide range of passing values, a weighed least squares scheme is often appropriate as ordinary least squares tend to match the coarse zone, since the absolute values of the error terms corresponding to them (and more so the squared ones) are much higher than those of the fines, which may be virtually neglected [12]. The weighting function depends on the range of sizes and passing of interest, and typically an inverse function of the size or the passing is used [12,55]. The form of the weighing function is

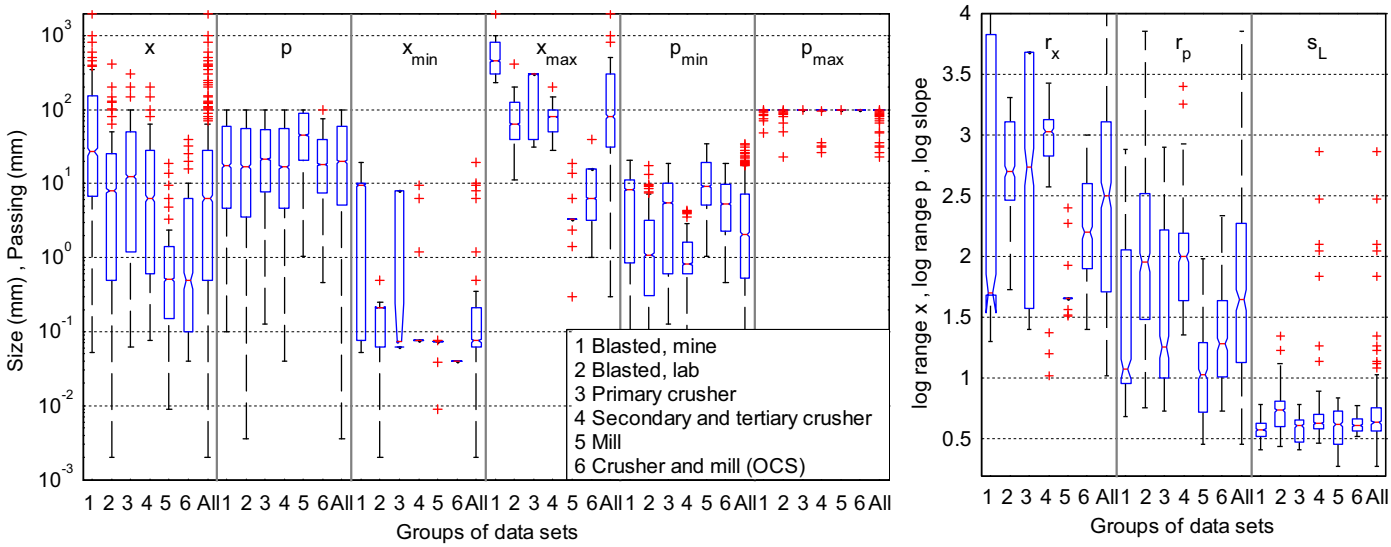

Fig. 2. Distributions of (left plot): global size and passing data, minimum and maximum size, minimum and maximum passing; (right plot): log size range, log passing range and overall log slope for the six groups in Table 1. The distributions for all the data sets are also shown. (For interpretation of the references to color in this figure, the reader is referred to the web version of this article.)

Table 2
Variables for which pairs of groups of data sets have statistically equal distributions to a 5% significance level.

	Group 1	Group 2	Group 3	Group 4	Group 5	Group 6
Group 1	All	p,p_{max}	p,p_{min},r_x,r_p,s_L	p,r_x	p_{min},s_L	p,p_{min},r_x,r_p
Group 2		All	r_x	x,p,x_{min},x_{max},p_{min},p_{max},r_p	x_{min}	p
Group 3			All	x_{min},x_{max},p_{max},r_x	x_{min},p_{max},s_L	p,p_{min},p_{max},r_p,s_L
Group 4				All	p_{max},s_L	p,p_{max},s_L
Group 5					All	x,x_{max},p_{max},s_L
Group 6						All

in itself an important subject [12] which, for the sake of conciseness, is not discussed in the present paper.

The fitting code has been programmed in Matlab [56] using non-linear function minimization routines. Two types of algorithms have been used:

(a) A Levenberg-Marquardt (L-M) algorithm with a trust-region reflective method [57,58]. No explicit Jacobian matrix is supplied to the algorithm, but it is estimated by finite differences. Even if reasonable bounds for the parameters (i.e. the variables to be solved in the minimization problem) could be established, the algorithm seems to perform better in finding new minima when no bounds are set. This better performance comes with the obvious penalty of calculating numerous solutions that include unfeasible values of the variables (e.g. negative characteristic size, or negative shape parameter), which are simply discarded. For each minimization problem, the maximum number of function evaluations used is $100 \times n_v$ and the maximum number of iterations is 400. Tolerances in function and variable values are 10^{-6}.

(b) A Nelder–Mead simplex search method. This is a direct search method [59] that does not use numerical or analytical gradients. It is essentially an unconstrained method so that the policy of discarding non-feasible solutions is put into practice here too. The maximum number of function evaluations used is $400 \times n_v$ and the maximum number of iterations is $200 \times n_v$. Tolerances in function and variable values are 10^{-4}.

The minimization problem, for virtually all the distribution functions, has proved to be prone to reaching local minima, regardless of the algorithm used to solve it. As such, the final minimum of the sum of squares, and the solution point, is very much dependent on the initial guess, this being especially true for functions of more than two parameters. In order to overcome this, each minimization problem (i.e. a data set and a distribution function) has been run repeatedly with different initial points, randomly generated within feasible intervals of the variables; filling of the n_v-dimensions initial points hypercubes in a log-uniform way has proved to be better than a (linear) uniform one. The number of minimizations finally used has been $1000 \times n_v$ (1000 times the number of parameters of the distribution function). The algorithm is assumed to have reached the global minimum when repeated minimizations (from different initial guess vectors) reach the same $\overline{\pi}$ solution and the same minimum of S within a given tolerance (relative difference of 10^5). Fig. 3 shows some examples of the progress of the calculation towards a global minimum as new minimization problems are run (the example corresponds to the fitting of the extended Swebrec distribution to twelve data sets with the direct search method).

Fig. 4 gives an overview of the number of minimizations required for the various distributions and minimization algorithms. Two-parameter distributions (WRR, GRA and LGN) require relatively few trials for the algorithm to reach a global minimum quite consistently. Three-parameter ones (SWE and GIL, especially the latter) require more trials until a global minimum can be ensured. Not surprisingly, the bi-component Gilvarry distribution (BiGIL), with seven parameters, requires effectively the highest number of minimization trials.

For most of the distributions, the performance of both optimization techniques is very similar in obtaining the global (or, at least, the "best") minimum of the squares sum; this is analyzed in Fig. 5 where the determination coefficient of the fits, R^2, is plotted.

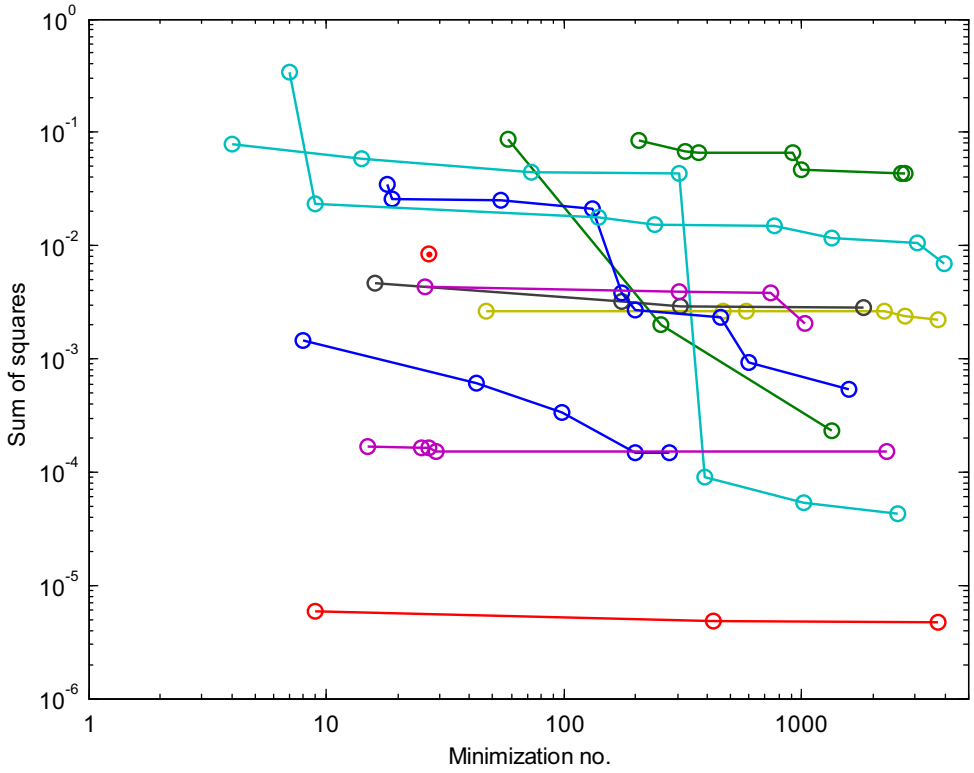

Fig. 3. Examples of progression of the minimization towards a global minimum. The vertical axis is the sum of squares S in Eq. (13).

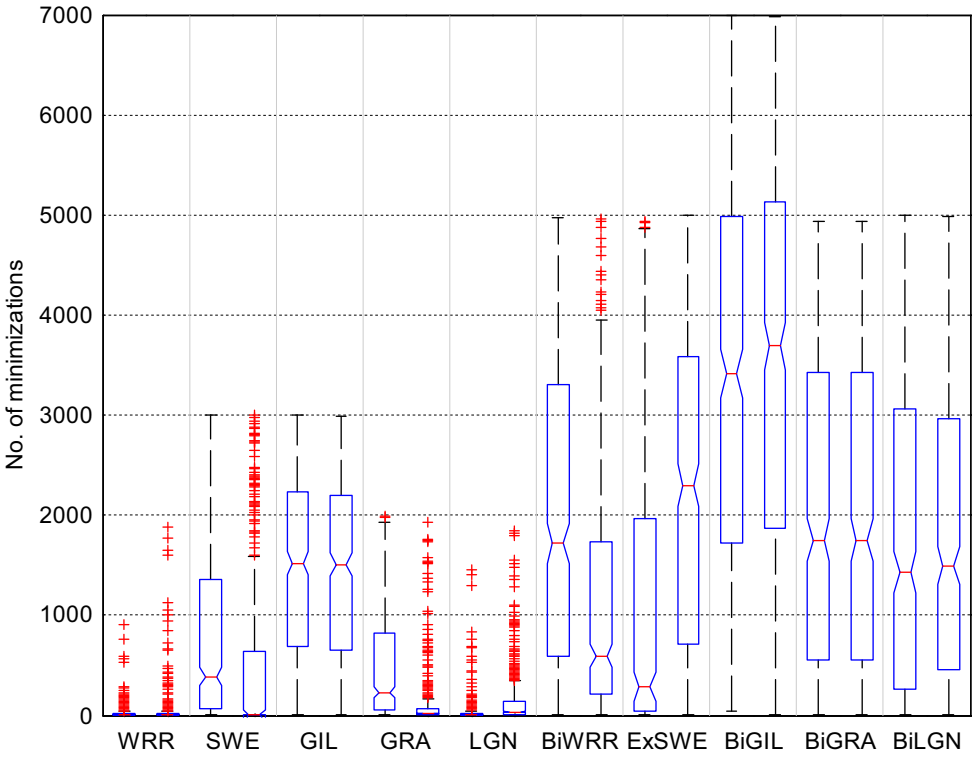

Fig. 4. Number of minimization problems solved. For each distribution function, left box: Levenberg-Marquardt; right box: simplex search.

The cases where there is a noticeable difference are the Swebrec and (less significant) the extended Swebrec, in favor of the L-M method. The number of trials required (Fig. 4) for the two minimization techniques is similar in some distributions (WRR, GIL, BiGIL, BiGRA, and BiLGN), while in others (SWE, GRA, and BiWRR) is higher for the L-M method, despite the similar value (except for the Swebrec case) of the minimum obtained. For the extended Swebrec, the number of minimizations are smaller with

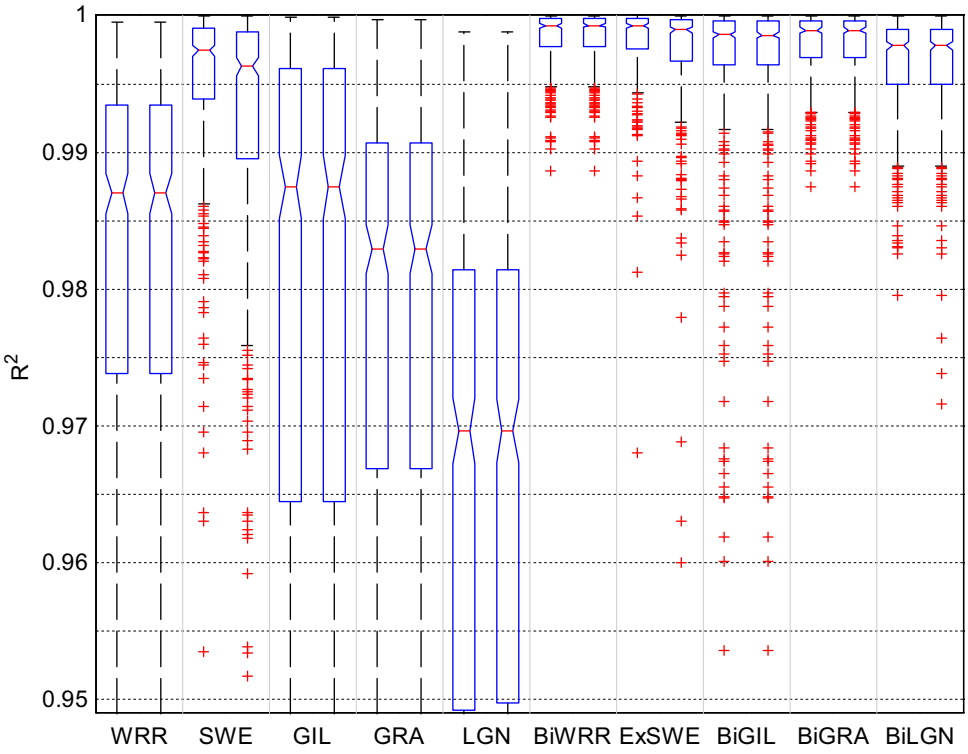

Fig. 5. Determination coefficient. For each distribution function, left box: Levenberg-Marquardt; right box: simplex search.

the L-M method than with the direct search (and, as mentioned before, with a lower minimum).

Regardless of the general rules above, some data sets are better fitted with one algorithm or the other. The particular characteristics of the data set have probably a bearing on that and no statement, other than the general experience cast in Figs. 4 and 5, can be made a priori on what algorithm will perform better with a particular set. In order to ensure that the target function (the sum of squares) reaches the best possible minimum in a massive fitting task as the one performed here, distributions have been fitted to all data sets with both methods, and the best solutions—the ones with smaller $S(\overline{\pi})$—have been retained.

Linearization of the functions is possible for the WRR and the Gilvarry cases. For the WRR, it can be done simply by a linear fit of $\ln(-\ln(1-p))$ to $\ln x$; for the Gilvarry, linearization leads to a multiple linear regression of $-\ln(1-p)$ against x, x^2 and x^3. The WRR fit proceeds fast and reliably towards a global minimum in fully non-linear form (as discussed above, see Fig. 4); also for the Gilvarry case, no significant improvement is obtained with the multiple linear fit in comparison to the fully non-linear scheme though in this case, being a three-parameter problem, the non-linear solution requires more calculation effort.

The quality of the fits has been assessed by means of the errors in calculating sizes; let x_p be the size at a percentage passing p in a given data set and x_p^* the size obtained from a given distribution function fitted to it, the relative error is

$$e_r = (x_p^* - x_p)/x_p \tag{14}$$

While the fitting has been carried out in the ordinary way of minimizing the residuals in the percentage passing (Eq. (13)), the assessment based on the errors in size has been chosen because it is easier to set a common group of passing values for all data sets on which to compare the corresponding sizes, than to set a common group of sizes on which to compare the corresponding passings. Besides, it has been felt that it is more practical to establish how well a size is determined at a given passing than how the passing is, since size estimation at a given passing is the typical result of fragmentation measurement and the preferred way of describing the fragmentation (e.g. what are the x_{50} or x_{80} values, or any other measure of the distribution location, scale, skewness, curtosis, etc.); sizes are involved in fragmentation prediction models and in the estimations of the work index for calculations of crushers energy and throughput [60]. The fitting could also have been carried out with a target of minimum error in size; this was however ruled out because of the asymptotic behavior at large x of most of the distributions tested (all except SWE and ExSWE); if the fit is to be performed in the space (p, x) with a criterion of least squared error in sizes, the calculated size at $p=1$ (or 100%) is infinite, so that the fit can only be done by rejecting the 100% point of the data set, or assuming a percentage passing close to 100% for it. Rejecting the upper point severely distorts the fitting in the coarse part, since the second point is often far below 100%; substituting the 100% value with an alternative one (e.g. 99.9, 99.99%,…) makes the result of the fitting dependent on what that value is.

In order to compare positive and negative errors at different passings and sizes in a fair way, logarithmic errors (which, unlike relative errors, are symmetric with respect to zero) have been used:

$$e_L = \ln(x_p^*/x_p) = \ln(e_r + 1) \tag{15}$$

To facilitate the comparison of errors, the original data are interpolated by Hermite polynomials (cubic polynomials matching the extremes of each data interval and with continuous derivative in those). The interpolation is done in log–log space with the support of p points spaced in such a way that the distribution of these replicates the distribution of passing points from all data sets; the x_p values are the interpolates for each support p point. This procedure allows the set of passing values used for the error calculations to be the same for all data sets

(within the passing range of each one). Fig. 6 shows, as a matter of illustration, the fits for one of the Bårarp's full scale blasts; the interpolated curve is the black solid line running through all data points (solid circles). Fig. 7 shows the log errors, calculated from Eq. (15), for the fits in Fig. 6. Two thousand passing values have been used for the support set so that the errors have a continuous-like appearance when plotted against the passing. Horizontal solid lines in Fig. 7 show the 100% error lines ($\pm \ln 2$).

5. Discussion

Though Figs. 6 and 7 are only an example, they show some of the general features of the fits; single component functions (except Swebrec) tend to fall steeply below 10%–20% passing whereas bi-components follow the data in a wider range. Consequently errors are, in general: (i) small in a central zone e.g. from 10% or 20% passing to about 80% or 90%; (ii) larger, though

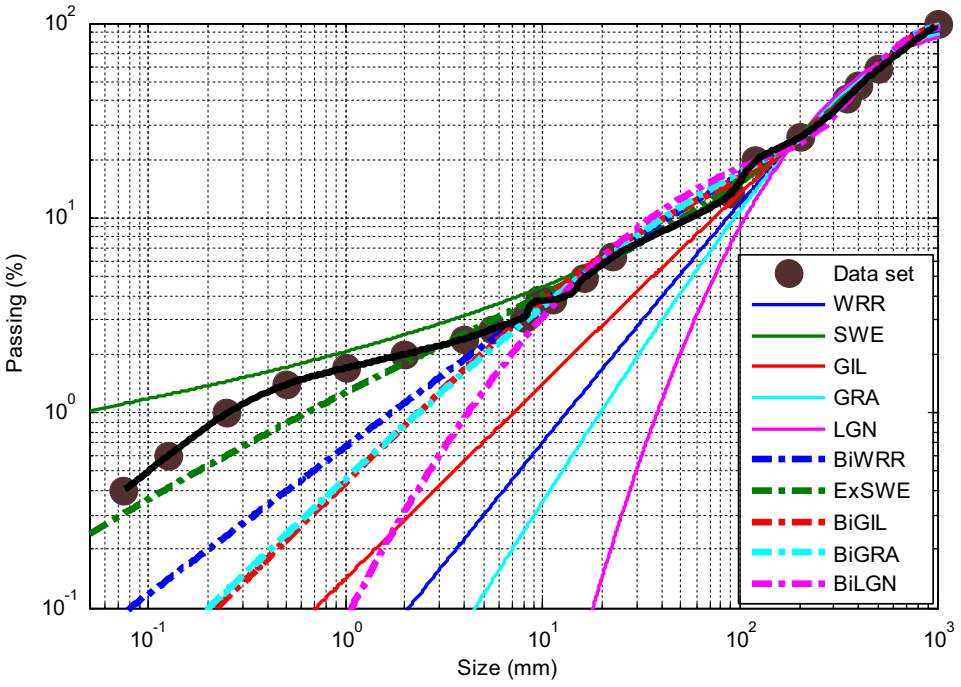

Fig. 6. Example of distribution functions fitted to a given data set; the black solid line running through all data points is the interpolated curve for error calculation purposes.

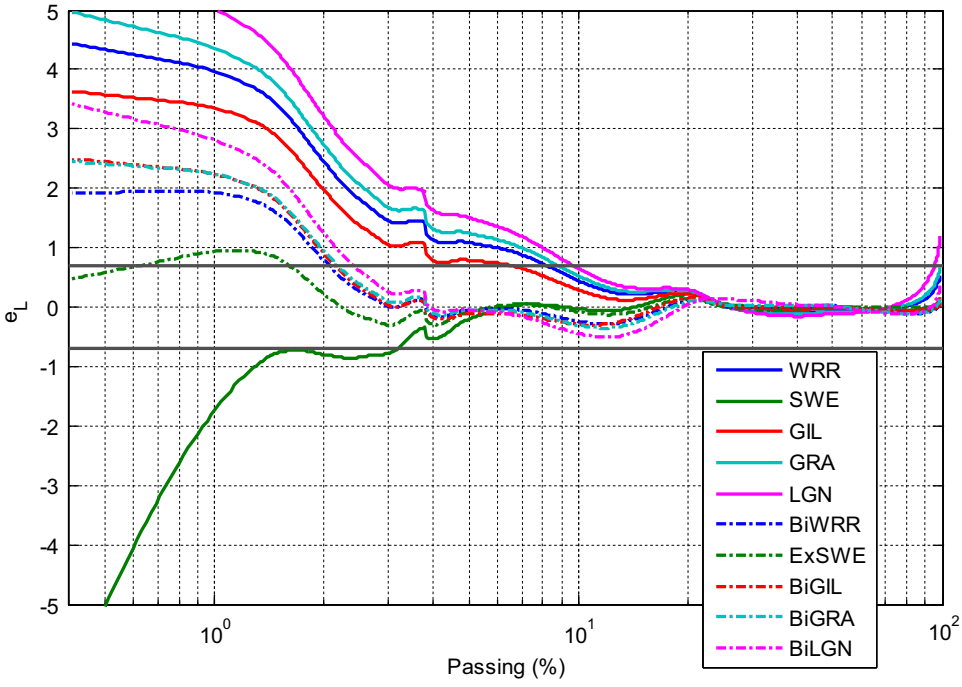

Fig. 7. Example of log errors.

relatively limited, near the upper passing extreme, and (iii) large at small passings (and, consequently, small sizes). Not all the distribution functions behave in the same way though in order to assess each function across the whole passing range, the distribution of the squared log errors, e_L^2, of each function for all the data sets at each passing value have been analyzed. Fig. 8 shows the root of the median and Fig. 9 the root of the 95 percentile of e_L^2 as functions of p.

By inspection of Figs. 8 and 9 it is again apparent that the uncontrolled behavior of the errors—both at the medians and at the 95% percentiles—below 10% or 20% passing, depending on the function, and also near 100% (for some functions, errors can be already in excess of 50% above 80% or 90%); Swebrec and extended Swebrec deviate from this behavior. For all distributions (though qualifications vary), the behavior is much better in the central zone.

Errors are generally higher in the single-component functions than in the two-component ones. This of course is something expected and consistent with what has been obtained about the determination coefficients (see Fig. 5). There is also some tangling of curves across the passing range and functions seem to behave differently in different passing zones. In order to explore this quantitatively, four zones of percentage passing have been defined: coarse ($p > 80\%$), central ($80\% > p > 20\%$), fine ($20\% > p > 2\%$) and very fine ($p < 2\%$).

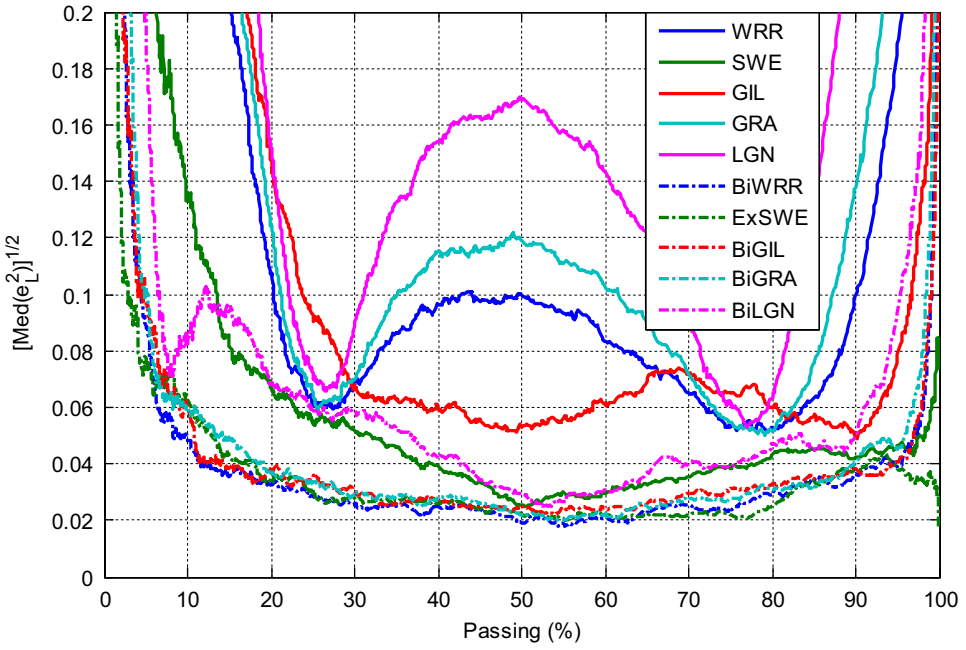

Fig. 8. Root of the medians of the squared log errors in size (e_L from Eq. (15)) of all data sets.

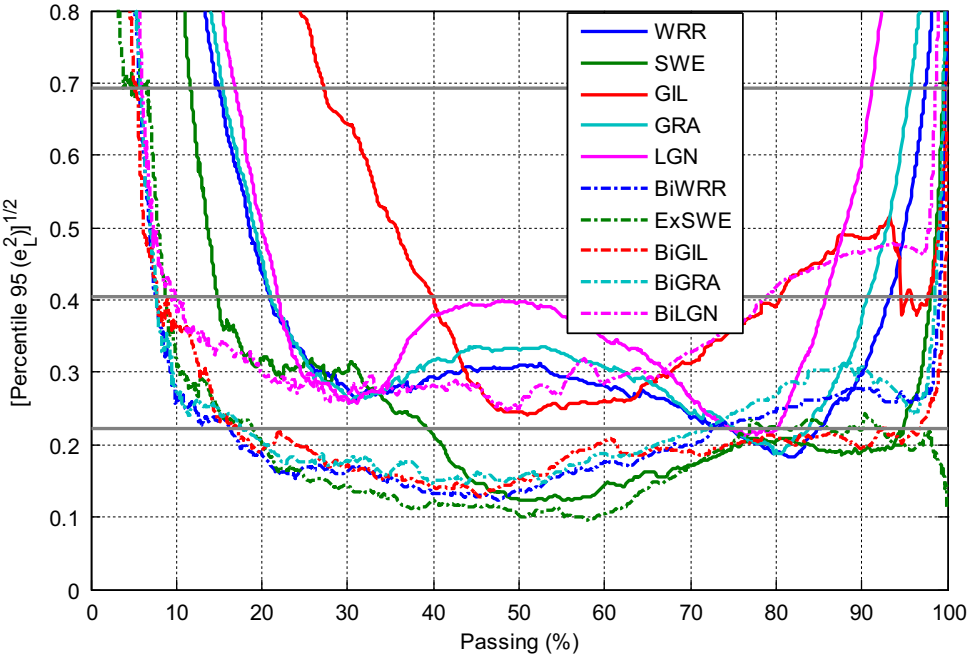

Fig. 9. Root of the 95% percentiles of the squared log errors in size (e_L from Eq. (15)) of all data sets. Horizontal lines show the 100%, 50% and 25% relative errors.

For each of these zones, a root mean squared log error has been calculated for each data set and fitting function, as follows:

$$RMSe_L = \left\{ \frac{1}{(p_s - p_i)} \int_{p_i}^{p_s} e_L^2 dp \right\}^{1/2} \tag{16}$$

where p_i and p_s are respectively the lower and upper limits of each passing zone. The p_i value for the very fines is the minimum passing, p_{min}, of each data set, and the p_s for the coarse is the maximum passing, p_{max}. If p_{min} and p_{max} are used together as p_i and p_s in Eq. (16), a global mean error is obtained for the whole passing range of the data set. The integrals are calculated numerically by the trapezoidal rule on the support set of p.

The distributions of $RMSe_L$ are given in Fig. 10. Errors for the four zones defined above and for the full range are shown. For each of them, the distributions of the errors for the ten functions tested are given in the form of box plots; solid circles are the 95 percentiles. As expected, two-component functions give smaller errors than single components, with relative errors in general less than 25% [i.e. log errors less than ln(1.25)], except in the very fine zone where errors, even for the best fitting functions can be very high. The 95 percentiles of the errors for the best fitting distributions are less than 25% for the coarse and central zones, and about 50% for the fine. Medians of errors are well below 10% for the best distributions (except, again, in the very fine zone).

Of the two-component functions, lognormal appears to be the worst in all zones, followed by Grady, while extended Swebrec seems to be the best fitting function in all zones: the median of ExSWE's $RMSe_L$ of all data sets is the lower in all passing zones, although in the central and fine the set of errors from some of the other functions cannot be said to be different than the ExSWE ones to a 0.05 significance (the Mann-Whitney test has been used, with the null hypothesis that the sets of errors of a pair of distributions belong to the same population); this is the case, for both central and fine zones, of BiWRR, BiGIL and BiGRA.

Among the single components, the Swebrec's $RMSe_L$ are comparable to the bi-components in the coarse and central zones; in the fine and very fine, its behavior is worse than any bi-component. Swebrec gives the lower errors of all single-component distributions in all zones. Errors of the WRR are significantly higher than SWE's everywhere, the best zone for WRR being the central. The fact that SWE has three parameters and WRR only two works in favor of obtaining lower errors with the former; however, GIL has also three parameters and its performance is not significantly better than WRR, and in some zones it is worse. WRR also outdoes the other two-parameter functions, GRA and LGN.

The good behavior of SWE in the coarse region is probably connected to the existence of a maximum size in this function, for which the percent passing is 100, as opposed to all other distributions; in the fines region, SWE's undulation characteristic, with a continuously decreasing slope towards small sizes (see Fig. 6), allows it to follow the data in a wider range than the exponentials (including the lognormal), which rapidly reach their small size slope and fall towards the fines much too steeply. This improved behavior of SWE in the fines in comparison with WRR has also been mentioned by Spathis [61].

In order to investigate a distinct behavior of the functions with fragmented materials of different origin, the number of data sets for which each function is the one with a lower $RMSe_L$ has been counted for each of the six groups of data (see Table 1a and 1b) and each passing zone. The result is plotted in Fig. 11, which shows the proportion (in percentage) of the data sets of a group for which a distribution gives the lower $RMSe_L$ for each passing zone. The global qualifications (all data sets considered) are also shown in the rightmost plot. Table 3 summarizes, for each data group and passing zone, the distributions with higher scores in Fig. 11. Functions quoted are those for which the null hypothesis

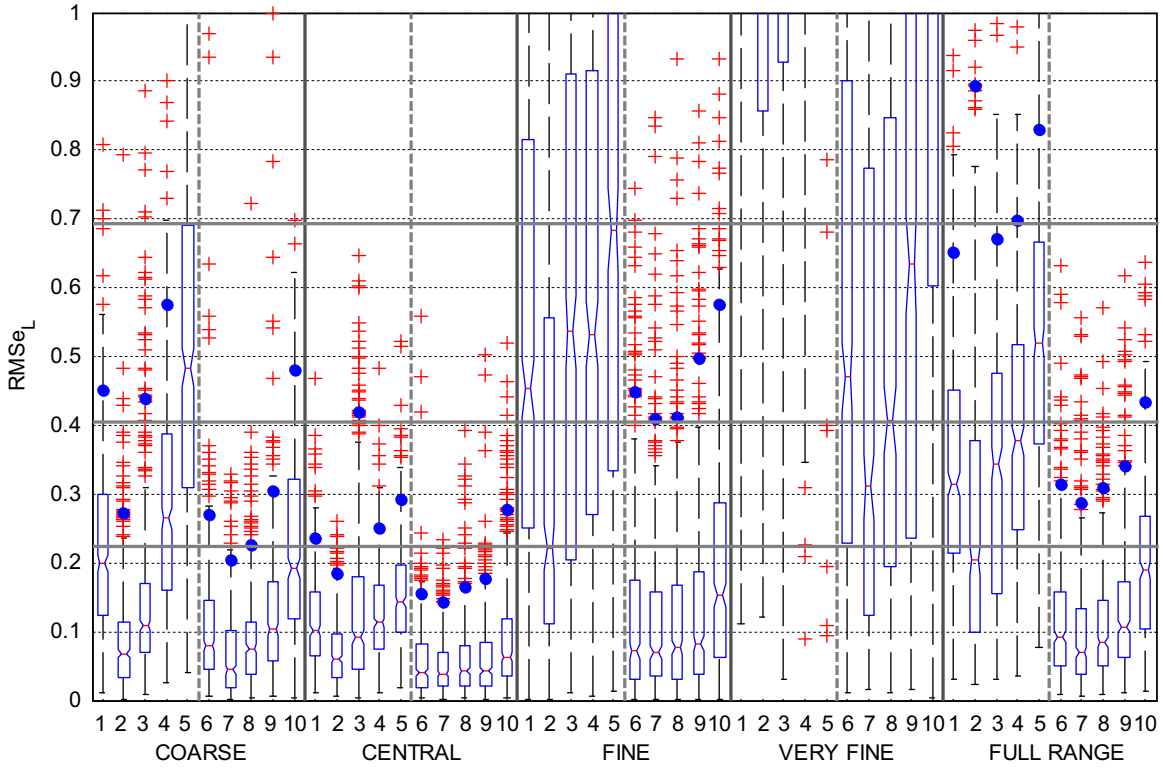

Fig. 10. Distributions of root mean squared errors for all data sets at different passing zones. Solid circles are the 95 percentiles. For each zone, left of the vertical dashed lines are the single-component functions (1–5) and right are the bi-component ones (6–10), in the following order: WRR, SWE, GIL, GRA, and LGN. Horizontal lines mark the 25%, 50% and 100% relative errors.

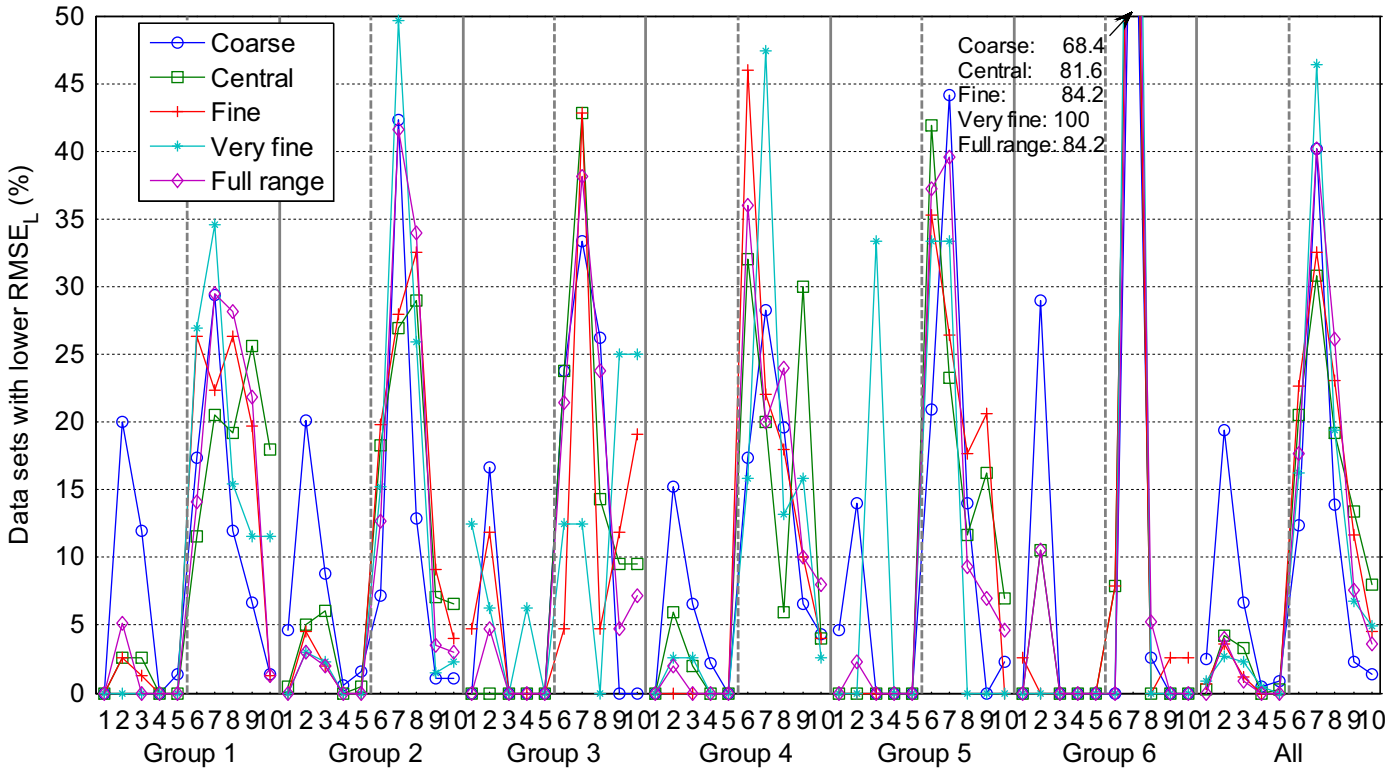

Fig. 11. Percentage of data sets of each group for which a given distribution gives a lower $RMSe_L$ in each passing zone. Groups 1 through 6 are as defined in Tables 1a and 1b. For each group, left of the vertical dashed lines are the single-component functions (1–5) and right are the bi-component ones (6–10), in the following order: WRR, SWE, GIL, GRA, and LGN.

that their proportions, treated as multinomial variables, are equal to the higher one is not rejected at a 0.05 significance. Confidence intervals for the difference of proportions have been determined by generating 2×10^5 random values of scores with probabilities equal to the proportions of each distribution for each data group and passing zone. The hypothesis of equal proportions is not rejected if the 95% coverage band for the difference includes zero. In some cases, when the number of data sets are small (such is the case for the very fines in groups 3 and 5), all functions may fail to reject that test, even if their scores are very low, or even zero; of course, the relevance of these figures is negligible. Such tests have also been performed using the Goodman–Bonferroni [62,63] intervals for the difference of multinomial proportions, with similar results for the groups with large number of data sets (about 100); for smaller groups the Goodman–Bonferroni confidence band is usually too wide, with actual coverage much higher than 95%; this was already recognized in [63]. Functions are listed in decreasing order of score; when the hypothesis of proportions equals to the best one is rejected for all the other functions, the second best is written in script; at the suggestion of an interested reviewer, the scores of WRR, SWE, BiWRR and ExSWE have been included in all the categories (in brackets when they are not in the best-scoring group).

The excellent performance of the extended Swebrec function across most of the data groups and passing zones is apparent. When all data sets are considered together, ExSWE is consistently the best scoring function in all passing zones. ExSWE is the best scoring for all data types in the coarse zone, though in some cases the scores of other functions are not rejected as being equal to a 0.05 significance. In the central zone, ExSWE is the best fitting for the primary crusher and OCS material and for other materials is within equal proportion hypothesis. The result is similar in the fine zone. In the very fine one—which cannot be said to be described properly by any function—ExSWE also does an acceptable job in most of the materials, in many groups being the highest score.

BiWRR is the best scoring function in the central and fine zones for secondary and tertiary crusher, and mill material, and also in the fine zone of mine blasted rock. It is within the hypothesis of equal score of the best function in many other materials and zones. It is the second global best score in the central zone.

The results of BiGIL, the function with a higher number of parameters (seven), are in general similar to BiWRR; it works well in the central and fine zones of blasted material (mine or lab) and in the coarse zone of crushed material; it is the overall second best scoring for fine and very fine material. Probably due to its seven parameters, it has a good score when the full passing range is considered, being the second function in blasted (mine and lab) and crushed materials, and also the second score when all data sets are considered.

As already mentioned around Fig. 10, SWE, a three-parameter function, does a very acceptable job in all materials, especially in the coarse zone, where it can compete with the errors of bimodal functions (with five or seven parameters); in the overall count, it is the second best-scoring function (after ExSWE) in that zone. It is also the second best in the coarse and central zones of laboratory crushed and ground (OCS) material.

6. Conclusions

Ten distributions, Weibull–Rosin–Rammler, Swebrec, Gilvarry, Grady and Lognormal, and their bi-component derivations, have been fitted to 448 sieved fragment size-passing data sets. The fits have been carried out with the ordinary minimum least squares criterion. Two minimization techniques have been applied: Levenberg-Marquardt and simplex direct search. In both cases,

Table 3
Performance for different types of data and passing zone. Figures in parentheses are the number of data sets for which the function has the lowest $RMSe_L$ in a given zone.

Group	Coarse	Central	Fine	Very fine	Full range
1 Blasted, mine	ExSWE (22) SWE (15) BiWRR (13) [WRR (0)]	BiGRA (20) ExSWE (16) BiGIL (15) BiLGN (14) [BiWRR (9)] [SWE (2)] [WRR (0)]	BiWRR (20) BiGIL (20) ExSWE (17) BiGRA (15) [SWE (2)] [WRR (0)]	ExSWE (9) BiWRR (7) BiGIL (4) BiGRA (3) BiLGN(3) [WRR (0)] [SWE (0)]	ExSWE (23) BiGIL (22) BiGRA (17) [BiWRR (11)] [SWE (4)] [WRR (0)]
No. of sets	75	78	76	26	78
2 Blasted, lab	ExSWE (82) *SWE (39)* [BiWRR (14)] [WRR (9)]	BiGIL (57) ExSWE (53) [BiWRR (36)] [SWE (10)] [WRR (1)]	BiGIL (64) ExSWE (55) [BiWRR (39)] [SWE (9)] [WRR (0)]	ExSWE (65) *BiGIL (34)* [BiWRR (20)] [SWE (4)] [WRR (0)]	ExSWE (82) BiGIL (67) [BiWRR (25)] [SWE (6)] [WRR (0)]
No. of sets	194	197	197	131	197
3 Primary crusher	ExSWE (14) BiGIL (11) BiWRR (10) SWE (7) [WRR (0)]	ExSWE (18) BiWRR (10) [WRR (0)] [SWE (0)]	ExSWE (18) BiLGN (8) [SWE (5)] [WRR (2)] [BiWRR (2)]	BiGRA (4) BiLGN (4) WRR (2) BiWRR (2) ExSWE (2) SWE (1) GRA (1)	ExSWE (16) BiGIL (10) BiWRR (9) [SWE (2)] [WRR (0)]
No. of sets	42	42	42	16	42
4 Secondary and tertiary crusher	ExSWE (13) BiGIL (9) BiWRR (8) SWE (7) [WRR (0)]	BiWRR (16) BiGRA (15) ExSWE (10) [SWE (3)] [WRR (0)]	BiWRR (23) *ExSWE (11)* [WRR (0)] [SWE (0)]	ExSWE (18) *BiWRR (6)* *BiGRA (6)* [SWE (1)] [WRR (0)]	BiWRR (18) BiGIL (12) ExSWE (10) [SWE (1)] [WRR (0)]
No. of sets	46	50	50	38	50
5 Mill	ExSWE (19) BiWRR (9) [SWE (6)] [WRR (2)]	BiWRR (18) ExSWE (10) [WRR (0)] [SWE (0)]	BiWRR (12) ExSWE (9) BiGRA (7) BiGIL (6) [WRR (0)] [SWE (0)]	GIL (1) BiWRR (1) ExSWE (1) [WRR (0)] [SWE (0)]	ExSWE (17) BiWRR (16) [SWE (1)] [WRR (0)]
No. of sets	43	43	34	3	43
6 Crusher and mill (OCS)	ExSWE (26) *SWE (11)* [BiWRR (0)] [WRR (0)]	ExSWE (31) *SWE (4)* [BiWRR (3)] [WRR (0)]	ExSWE (32) *BiWRR (3)* [WRR (1)] [SWE (0)]	ExSWE (8) [WRR (0)] [SWE (0)] [BiWRR (0)]	ExSWE (32) *SWE (4)* [WRR (0)] [BiWRR (0)]
No. of sets	38	38	38	8	38
All	ExSWE (176) *SWE (85)* [BiWRR (54)] [WRR (11)]	ExSWE (138) *BiWRR (92)* [SWE (19)] [WRR (1)]	ExSWE (142) *BiGIL (101)* [BiWRR (99)] [SWE (16)] [WRR (3)]	ExSWE (103) *BiGIL (43)* [BiWRR (36)] [SWE (6)] [WRR (2)]	ExSWE (180) *BiGIL (117)* [BiWRR (79)] [SWE (18)] [WRR (3)]
No. of sets	438	448	437	222	448

the solution is dependent on the initial values assigned to the model parameters, especially for problems with more than two unknowns, so that a scheme of multiple initial points is imperative to ensure a global minimum; safe results have been obtained with a maximum number of trials (with different initial points randomly generated within feasible bounds) 1000 times the number of unknowns. There does not appear to be a significant difference on the minimum obtained and the number of trials required with both minimization techniques; some preference for the Levenberg-Marquardt method appears in the Swebrec fitting and also (though minor) in the extended Swebrec.

The quality of the fits have been explored in terms of logarithmic errors in the prediction of the size at a given passing value, which have been calculated for all data sets and distributions fitted across their whole passing ranges.

A general rule is that the representation of the experimental fragmentation data can be very accurate (with variations for different functions though) in a central zone, defined from about 20% to 80% passing. Errors tend to increase towards the upper end of the curves in the functions with an asymptote at 100% passing while they stay relatively contained with the functions that include a (x_{max}, 100) point (Swebrec and extended Swebrec). Towards the fines side, errors increase consistently with all distribution functions, moderately down to percentages passing of around a few units, and totally out of control below that. Four zones have been defined for the analysis of the errors: coarse (passing above 80%), central (80% to 20%), fine (20% to 2%) and very fine (below 2%).

The behavior of the distributions in the different zones has been assessed by the root mean squared logarithmic error in each

of the above zones for each distribution and data set. It has been found that errors can be (in terms of the median of all data sets, expressed as relative errors) as low as less than 5% for some distributions in the coarse and central zones and less than 10% in the fine zone. For the very fines, the lower median error is less than 50% in the best case, though the distribution of errors is very wide, encompassing very large values. In terms of the 95 percentiles, errors are less than 25% in the coarse and central zones for the best fitting distributions, hardly less than 50% for the fine zone, and beyond any reasonably acceptable value, even for the best fitting distribution, in the very fine zone.

Bi-component distributions generally perform a better fit, as should be expected, though there are important differences among them. Extended Swebrec is consistently the best fitting distribution in all zones, including the full range: maximum errors expected for it (estimated as the 95 percentiles) are less than 25% in the coarse, 15% in the central and 50% in the fine zones. Bimodal Weibull, bimodal Gilvarry and bimodal Grady's errors are statistically equivalent to extended Swebrec's in the central and fine zones. In the very fines, errors have a high probability of being in excess of 100% (all third quartiles are higher than that), with maximum expected, even for the best fitting functions in this zone—extended Swebrec, bimodal Gilvarry and bimodal Weibull—completely out of control (95 percentiles of log errors are around 2 or 2.5, that correspond to relative errors around 1000%). This tells that the extrapolation capacity towards the very fine sizes of any distribution, when fits are carried out with an OLS criterion to the full size span, is limited, and that any quantitative statement based on extrapolations below passings of 1% or 2% is extremely risky.

The behavior of the Swebrec—a three parameter distribution—is comparable to the best bi-components in the coarse and central zones, and it is the best fitting single component distribution in all passing zones; errors of the Weibull–Rosin–Rammler distribution are about double than Swebrec's in all zones.

Acknowledgments

We would like to thank Claude Cunningham and Cameron McKenzie for kindly providing unpublished fragmentation data.

References

[1] King RP. Modeling and simulation of mineral processing systems. Oxford: Butterworth-Heinemann; 2001.
[2] Gupta A, Yan DS. Mineral processing design and operations. Amsterdam: Elsevier; 2006.
[3] Cunningham CVB. The Kuz-Ram model for prediction of fragmentation from blasting. In: Proceedings of the 1st international symposium on rock fragmentation by blasting. Lulea, Sweden, 22–26 August 1983, p. 439–52.
[4] Cunningham CVB. Fragmentation estimations and the Kuz-Ram model—four years on. In: Proceedings of the 2nd international symposium on rock fragmentation by blasting. Keystone, Colorado, USA, 23–26 August 1987, p. 475–87.
[5] Ouchterlony F, Niklasson B, Abrahamsson S. Fragmentation monitoring of production blasts at MRICA. In: Proceedings of the 3rd international symposium on rock fragmentation by blasting. Brisbane, Australia, 26–31 August 1990, p. 283–9.
[6] Otterness RE, Stagg MS, Rholl SA, Smith NS. Correlation of shot design parameters to fragmentation. In: Proceedings of the 7th annual symposium on explosives and blasting research. Las Vegas, Nevada, USA, 6–7 February 1991, p. 179–90.
[7] Kou S, Rustan A. Computerized design and result prediction of bench blasting. In: Rossmanith HP, editor. Proceedings of the 4th international symposium on rock fragmentation by blasting. Vienna, 5–8 July 1993, p. 263–71.
[8] Djordjevic N. Two-component model of blast fragmentation. In: Proceedings of the 6th International symposium on rock fragmentation by blasting. Johannesburg, South Africa, 8–12 August 1999, p. 213–9.
[9] Kanchibotla SS, Valery W, Morrell S. Modelling fines in blast fragmentation and its impact on crushing and grinding. In: Proceedings of the Explo'99—a conference on rock breaking. Kalgoorlie, Australia, 7–11 November 1999, p. 137–44.
[10] Chung SH, Katsabanis PD. Fragmentation prediction using improved engineering formulae. Int J Blasting Fragmentation 2000;4(3–4):198–207.
[11] Thornton DM, Kanchibotla SS, Esterle JS. A fragmentation model to estimate ROM size distribution of soft rock types. In: Proceedings of the 27th annual conference on explosives and blasting technique. Orlando, Florida, 28–31 January 2001, p. 41–53.
[12] Sanchidrián JA, Ouchterlony F, Segarra P, Moser P, López LM. Evaluation of some distribution functions for describing rock fragmentation data. In: Sanchidrián JA, editor. Proceedings of the 9th international symposium on rock fragmentation by blasting (Fragblast 9). Granada, Spain, 13–17 September 2009. Leiden: CRC Press/Balkema. p. 239–48.
[13] Rosin P, Rammler E. The laws governing the fineness of powdered coal. J Inst Fuel 1933;7:29–36.
[14] Weibull W. A statistical theory of the strength of materials. Ingeniörsvetenskapsakad Handl 1939;151:1–45.
[15] Weibull W. A statistical distribution function of wide applicability. J Appl Mech ASME 1951;18:293–7.
[16] Ouchterlony F. The Swebrec© function, linking fragmentation by blasting and crushing. Mining Technology (Trans Inst Min Metall Sect A) 2005;114: A29–A44.
[17] Ouchterlony F. What does the fragment size distribution of blasted rock look like? In: Holmberg R, editor. Proceedings of the 3rd world conference on explosives and blasting. Brighton, 13–16 September 2005, p. 189–99.
[18] Gilvarry JJ. Fracture of brittle solids. I. Distribution function for fragment size in single fracture (theoretical). J Appl Phys 1961;32(3):391–9.
[19] Gilvarry JJ, Bergstrom BH. Fracture of brittle solids. II. Distribution function for fragment size in single fracture (experimental). J Appl Phys 1961;32(3): 400–410.
[20] Sil'vestrov VV. Fragmentation of a steel sphere under a high-velocity impact on a highly porous thin bumper. Combust Explos Shock Waves 2004;40(2): 238–252.
[21] Sil'vestrov VV. Application of the Gilvarry distribution to the statistical description of fragmentation of solids under dynamic loading. Combust Explos Shock Waves 2004;40(2):225–37.
[22] Grady DE, Kipp ME. Geometric statistics and dynamic fragmentation. J Appl Phys 1985;58(3):1210–22.
[23] Grady DE. Particle size statistics in dynamic fragmentation. J Appl Phys 1990;68(12):6099–105.
[24] Kutter HK, Fairhurst C. On the fracture process in blasting. Int J Rock Mech Min Sci Geomech Abstr 1971;8(3):181–202.
[25] Fourney WL, Holloway DC, Wilson WH, Barker DB. Fragmentation studies in jointed brittle material. In: Fourney WL, Boade RR, Costin LS, editors. Fragmentation by blasting. Bethel, CT: Society for Experimental Mechanics; 1985. p. 73–87.
[26] Åström JA, Linna RP, Timonen J, Møller PF, Oddershede L. Exponential and power-law mass distributions in brittle fragmentation. Phys Rev 2004;E70: 026104.
[27] Åström JA, Ouchterlony F, Linna RP, Timonen J. Universal dynamic fragmentation in D dimensions. Phys Rev Lett 2004;92(24):245506.
[28] Blair DP. Curve-fitting schemes for fragmentation data. Int J Blasting Fragmentation 2004;8(3):137–50.
[29] Sanchidrián JA, Segarra P, Ouchterlony F, López LM. On the accuracy of fragment size measurement by image analysis in combination with some distribution functions. Rock Mech Rock Eng 2009;42(1):95–116.
[30] Sanchidrián JA, Segarra P, López LM. A practical procedure for the measurement of fragmentation by blasting by image analysis. Rock Mech Rock Eng 2006;39(4):359–82.
[31] Bond FC, Whitney BB. The work index in blasting. Q Colo Sch Mines 1959; 54(3):77–82.
[32] McKenzie C. Personal communication; 2003.
[33] Olsson M, Bergqvist I. Fragmentation in quarries. In: Proceedings of the Disc Meeting BK 2002, Swedish Rock Construction Committee. Stockholm, Sweden, 2002, p. 33–8 [in Swedish].
[34] Gynnemo M. Investigation of governing factors in bench blasting. Full-scale tests at Kållered and Billingsryd. Publ. A84. Gothenburg, Sweden: Chalmers University, Department of Geology; 1997 [in Swedish].
[35] Cunningham CVB. Personal communication; 2003.
[36] Grimshaw HC. The fragmentation produced by explosive detonated in stone blocks. In: Walton WH, editor. Mechanical properties of non-metallic brittle materials. Proceedings of a conference on non-metallic brittle materials. London, April 1958. London: Butterworth. p. 380–8.
[37] Moser P, Grasedieck A, Arsic V, Reichholf G. Charakteristik der Korngrössenverteilung von Sprenghauwerk im Feinbereich. Berg Hüttenmänn Monatsh 2003;148:205–16 [in German].
[38] Moser P, Grasedieck A, du Mouza J, Hamdi E. Breakage energy in rock blasting. In: Holmberg R, editor. Proceedings of the 2nd world conference on explosives and blasting. Prague, 10–12 September 2003. Rotterdam: Balkema. p. 323–34.
[39] Moser P, Grasedieck A, Olsson M, Ouchterlony F. Comparison of the blast fragmentation from lab-scale and full-scale tests at Bårarp. In: Holmberg R, editor. Proceedings of the 2nd world conference on explosives and blasting. Prague, 10–12 September 2003. Rotterdam: Balkema, p. 449–58.
[40] Kristiansen J. Blastability of rock, small-scale tests in rock blocks. Report no. 548095-4. Oslo: Norwegian Geotech Inst; 1994 [in Norwegian].

[41] Kristiansen J. Blastability of rock, full-scale blasting tests with different hole diameters. Report no. 548095-5. Oslo: Norwegian Geotech Inst; 1995 [in Norwegian].
[42] Rustan A, Naarttijärvi T. The influence from specific charge and geometric scale on fragmentation. Report no. FG8322. Luleå, Sweden: Swedish Mining Research Foundation; 1983.
[43] Svahn V. Generation of fines around a borehole: a laboratory study. In: Proceedings of the 7th international symposium on rock fragmentation by blasting. Beijing, 11–15 August 2002. Beijing: Metallurgical Industry Press, p. 122–27.
[44] Svahn V. Generation of fines in bench blasting. Licenciate thesis, Pub. A104. Gothenburg, Sweden: Chalmers University, Department of Geology; 2003.
[45] Hänninger A, Larsson L, Slokenbergs M. Investigation of results and capacities when crushing andesite. Diploma thesis no. 308. Hydraulics Lab, Stockholm: Royal Institute of Technology; 1988 [in Swedish].
[46] Moser P. Less fines production in aggregate and industrial minerals industry. In: Holmberg R, editor. Proceedings of the 2nd world conference on explosives and blasting. Prague, 10–12 September 2003. Rotterdam: Balkema, p. 335–43.
[47] Napier-Munn TJ, Morell S, Morrison RD, Kojovic T. Mineral comminution circuits—their operation and optimisation. In: Proceedings of the JKMRC monograph series in mining and mineral processing. Indooroopilly, Queensland, Australia; 1996.
[48] Kristiansen J. A study of how the velocity of detonation affects fragmentation and the quality of fragments in a muckpile. In: Proceedings of the Explo'95. Publication series no. 6/95. Carlton, Vic., Australia: AusIMM; 1995, p. 437–44.
[49] Chi G. A study of comminution efficiency in relation to controlled blasting in mining. PhD thesis. Reno: University of Nevada; 1994.
[50] Chi G, Fuerstenau MC, Bradt RC, Ghosh A. Improved comminution efficiency through controlled blasting during mining. Int J Miner Process 1996;47:93–101.
[51] Fuerstenau MC, Chi G, Bradt RC, Ghosh A. Increased ore grindability and plant throughput with controlled blasting. Min Eng 1997;49(12):70–5.
[52] Leoben MU. The natural breakage characteristics (NBC) and energy register functions for the rock mass of the quarries Nordkalk, Cementos Portland and Hengl Bitustein. Less fines, EU Project GRD-2000-25224, Tech. Rep. 33; 2002.
[53] Steiner HJ. The significance of the Rittinger equation in present-day comminution technology. In: Proceedings of the international mineral processing congress. Dresden, Germany, 1991, vol. I, p. 177–88.
[54] Hollander M, Wolfe DA. Nonparametric statistical methods. Hoboken, NJ: John Wiley & Sons; 1999 p. 106–25.
[55] Ouchterlony F. Fragmentation characterization, the Swebrec function and its use in blast engineering. In: Sanchidrián JA, editor. Proceedings of the 9th international symposium on rock fragmentation by blasting (Fragblast 9). Granada, Spain, 13–17 September 2009. Leiden: CRC Press/Balkema. p. 3–22.
[56] Matlab 7.13. Natick, MA: The MathWorks Inc; 2011.
[57] Coleman TF, Li Y. On the convergence of reflective Newton methods for large-scale nonlinear minimization subject to bounds. Math Program 1994;67(2): 189–224.
[58] Coleman TF, Li Y. An interior, trust region approach for nonlinear minimization subject to bounds. SIAM J Optim 1996;6(2):418–45.
[59] Lagarias JC, Reeds JA, Wright MH, Wright PE. Convergence properties of the Nelder-Mead Simplex method in low dimensions. SIAM J Optim 1998;9(1): 112–147.
[60] Bond FC. The third theory of comminution. Trans AIME 1952;193:484–94.
[61] Spathis AT. Formulae and techniques for assessing features of blast-induced fragmentation distributions. In: Sanchidrián JA, editor. Proceedings of the 9th international symposium on rock fragmentation by blasting (Fragblast 9). Granada, Spain, 13–17 September 2009. Leiden: CRC Press/Balkema. p. 209–19.
[62] Goodman LA. On simultaneous confidence intervals for multinomial proportions. Technometrics 1965;7(2):247–54.
[63] Piegorsch WW, Richwine KA. Large-sample pairwise comparisons among multinomial proportions with an application to analysis of mutant spectra. J Agric Biol Environ Stat 2001;6(3):305–25.